STM JOURNALS

Journal of
Remote Sensing & GIS

ISSN: 2230-7990 (Online)
ISSN: 2321-421X (Print)
Volume 14, Issue 1, 2023
DOI (Journal): 10.37591/JoRSG

http://techjournals.stmjournals.in/index.php/JoRSG/index

Research JoRSG

Sensitivity Analysis of a Sky Wave Over-the-Horizon Radar Simulation Tool

Zenon Saavedra[1], Adrian Llanes[2], Gonzalo Alderete Hero[2], Blas de Haro Barbas[1], Julian Di Venanzio[3], Ana G. Elias[2,*]

Abstract

A simulation tool of a sky wave over-the-horizon radar performance and detection process includes many stages based on different models, which creates a synthetic searching scenario as a first step followed by a digital signal processing to detect and locate a potential target. Its accuracy will depend on the quality of the input and adequacy degree of the model assumptions. A sensitivity analysis of this simulation tool is carried out analyzing outputs' variation as a consequence of changes in input factors. The architecture of this tool allow easy implementation and the study of input variables impact on detection and location results that can be useful towards dimensioning features and elements of a real radar.

Keywords: Over-the-horizon radar, simulation, sensitivity analysis, Doppler frequency

INTRODUCTION

A sky-wave over-the-horizon radar (OTHR) is a long-range beyond horizon radar system suitable for wide-area surveillance of aircrafts and maritime vessels [1], which works in the high frequency (HF) range of electromagnetic waves, that is in the 3–30 MHz frequency range. This radar signal travel through the ionosphere to and from a searching area, in order to detect, locate and eventually track a possible target in this region. Doppler shift measurements of this signal is used to differentiate between echoes coming from moving targets and those from ground and sea surfaces. The whole process involves several connected physical mechanisms which depend on OTHR specific properties. They can be modeled as quasi-independent blocks to analyze synthetic scenarios in order to define and select the radar's characteristics, parameters and range of operation which are essential to achieve the best performance [2, 3].

***Author for Correspondence**
Ana G. Elias
E-mail: aelias@herrera.unt.edu.ar

[1]Professor, Faculty of Exact Sciences and Technology (FACET), Department of Physics, National University of Tucuman, Tucuman (UNT), Argentina & CONICET
[2]PhD Student, Faculty of Exact Sciences and Technology (FACET), National University of Tucuman (UNT), Tucuman, Argentina
[3]General Directorate for Research and Development, Air Force Argentina (FAA)

Received Date: February 16, 2023
Accepted Date: March 18, 2023
Published Date: March 25, 2023

Citation: Zenon Saavedra, Adrian Llanes, Gonzalo Alderete Hero, Blas de Haro Barbas, Julian Di Venanzio, Ana G. Elias. Sensitivity Analysis of a Sky Wave Over-the-Horizon Radar Simulation Tool. Journal of Remote Sensing & GIS. 2023; 14(1): 20–30p.

In the present work, a sensitivity analysis (SA) of the OTHR simulation tool described in Saavedra et al. [4, 5] is made to evaluate this kind of radar behavior and performance according to a given set of input parameters. SA arises as a fundamental approach to reach this goal, since it consists on the investigation of how the variation in the output of a decision-making or modeling process can be attributed to variations in the different input factors, together with the importance of uncertainties in model inputs and assumptions [6, 7]. This work is organized as follows. The general aspects of the OTHR simulation tool considered are described first in Section 2. The variable parameters and the SA results are analyzed in Section 3, followed by the discussion and conclusions in Section 4.

OTHR SIMULATION TOOL DESCRIPTION

The OTHR simulation tool considered in this work [4, 5] performs the whole process from the transmitter and signal generation to the target location and detection in a range-Doppler spectrum, as shown schematically in Figure 1. The "parameters setup" block is common to many phases in the simulation, where input parameters are selected which define the characteristics of the radar, search scenario and target to be detected. A list of them and their values for a given example can be seen in Tables 1, 2 and 3.

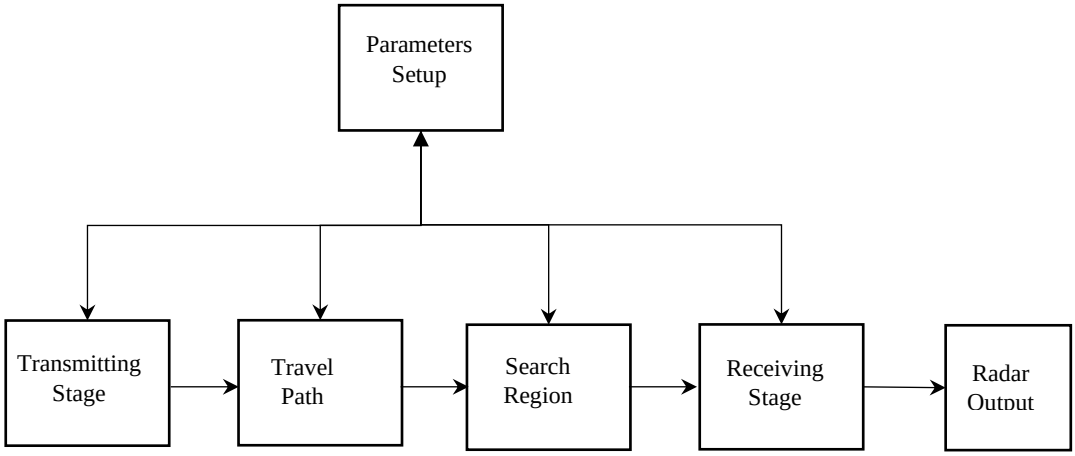

Figure 1. Block diagram of the Over-The-Horizon Radar (OTHR) simulation computer code indicating each block function.

Table 1. Transmitter specifications including transmitted signal characteristics.

Transmitter Parameters	**Value**
Geographic position	42.3ºS 63.8ºW
Altitude	0 km (sea level)
Carrier Frequency (f_C)	6 MHz
Polarization	Horizontal
Bandwidth (B)	10 kHz
Elevation Angle (α)	3º to 9º
Elevation angle Beamwidth	1º
Azimuth Angle (φ)	98º
Azimuth angle Beamwidth	3º
Transmitted Power (P_T)	500 kW
Antenna's gain Tx	20 dB
Antenna's gain Rx	25 dB

Table 2. Environmental specifications.

Environment Parameter	**Value**
Date	June 15, 2010
Local time	3:00 PM
Sea state [0 to 8]	5 (moderate)
Sea radar cross section (σ_C)	68 dBsm
Bragg frequency (for f_c = 6 MHz) (f_B)	0.25 Hz
Loss	-345 dB

Table 3. Target specifications.

Target Parameters	Value
Geographic position	42.58°S, 45.18°W
Distance from transmitter	1400 km
Speed	15 km/h
Doppler frequency (for f_c = 6 MHz) (f_D)	0.167 Hz
Type	Fishing vessel
Aspect angle	90 º
Radar cross section (σ_T)	35 dBsm
Geographic position	42.58º S, 45.18º E $R_{target} = 1400$ km.

Transmitting Stage

The operation mode of the radar transmitter and waveform of the transmitted signal are defined in this block. A monostatic radar in which the transmitter and receiver are collocated is considered. The specifications that define this system in our simulation are: carrier frequency (f_c), bandwidth (B), polarization, transmitted power (P_T), transmitter gain (G_T) and receiver gain (G_R). For location purposes geographic location, altitude, elevation angle, and azimuth are also specified. All these parameters are defined in the parameters setup block.

Since transmitter and receiver are collocated a pulsed waveform is considered for the transmitted signal, $S_T(t)$, of pulse time length T and a pulse repetition frequency PRF. For its bandwidth (B), taking into account that in general the ionosphere effectively supports bandwidths of a few tenths of kHz [8], a typical value of B = 10 kHz is considered for this simulation.

$S_T(t)$ is given by

$$S_T(t) = u(t)\, P_T\, G_T\, m(t)\, e^{j2\pi f_c t+\varphi} \quad (1)$$

where u(t) is a square pulse envelope of amplitude 1 and duration T, m(t) is the modulation type for pulse compression, and φ is the signal phase. Either frequency or phase modulation m(t) can be set for pulse compression. The options for each of them in this simulation tool are: linear frequency modulation (LFM) in the first case, and binary phase (BPSK) and polyphase modulation in the latter.

Travel Path

The interaction between the electromagnetic wave and propagation channel is considered in this block, which can be separated in three smaller blocks: propagation path model, attenuation and coordinate registration.

The signal propagation path is estimated with the Jones & Stephenson ray tracing code [9], implemented as an independent block. This code has options for: (1) the electron density profile, which can be chosen from two analytical models or the IRI-2016 model [10], (2) the Earth's magnetic field from the IGRF-12 model [11], which can be turned on and off, and (3) collision frequencies, which can also be turned on and off. From this ray tracing we obtain the two-way delay of the signal travelling between the transmitter and the target, τ_R, the target ground range distance, D, and azimuth relative to the transmitter.

Attenuation, or loss, is a reduction in power that results from absorption along the propagation path or radar components. The most significant are geometric, deviative and non-deviative attenuations. The first one, L_g, corresponds to the loss of energy due to its distribution over the spherical surface and is estimated in dB as $L_g = 20 \log(S)$, where S is the complete path length covered by the ray [12],

and is obtained from the propagation path model. The deviative attenuation, L_d, is due to the portion of the radio path in the ionosphere close to the point of reflection. It is usually small and will be neglected here. Non-deviative attenuation, L_{nd}, is mainly due to the ray path through the lowest ionospheric layers that D and E regions, and can be approximated in dB/km by Equation (20) in Recommendation ITU-R P.533-13 publication [13, 11].

The coordinate registration (CR) process converts the group range and azimuth of each scanned cell that is obtained with the ray tracing code, into geographic coordinates (longitude and latitude) based in a simplified geometric analysis. The propagation path accuracy along the ionosphere will define CR precision.

Search Region

This block considers the interaction among the electromagnetic wave, the environment and the target to be detected. It includes the cross section models of the target and the sea clutter.

The electromagnetic simulations software CST (Computer Simulation Technology) Microwave Studio was used to estimate the target radar cross section, σ_T. The inputs needed are obtained from a 3-D CAD model of the target, together with the materials of which the object is composed. σ_T is then obtained as a function of carrier frequency and polarization. To consider σ_T fluctuations Swerling models 1 to 4 can be selected.

Only a small fraction of the transmitted electromagnetic energy impacts on the target, and most of it impacts over the sea. The return of the latter is an unwanted signal and constitutes sea clutter that is obtained from

$$\sigma_C = \sigma_0 \, A \tag{2}$$

where σ_C is the clutter radar cross section, σ_0 is the scattering coefficient, and A is the area of the scattering patch. Even though σ_0 depends on the radio wave polarization, frequency, angle of incidence and sea surface conditions (or "roughness"), typical mean values obtained from tables are assumed [1]. Three different options for PDF are included: K-distribution, Lognormal, and Rayleigh type [14].

Receiving Stage

This block handles the received synthetized signals and a chain of digital processing applied to it in order to detect a target. The main aspects of this block are the following.

$S_T(t)$ is received back by the radar receiver after being scattered, not only by the target, but other sources as well. We will consider a received signal, $S_R(t)$, given by

$$S_R(t) = S_{Echo}(t) + S_{Noise}(t) + S_{Clutter}(t) \tag{3}$$

where $S_{Echo}(t)$, $S_{Noise}(t)$, and $S_{Clutter}(t)$ are the signals reaching the receiver emitted by the target, and unwanted noise and clutter, respectively.

Considering a moving target with velocity v along the radar light of sight, S_{Echo} results

$$S_{Echo}(t) = A \, \sigma_T \, P_T \, G_R \, G_T \, u(t - \tau_R) \, m(t) \, e^{j\omega_C t \pm j\omega_D t} \tag{4}$$

where ω_D is the target Doppler frequency ($\omega_c v/c$), c is the light velocity, and A is the two-way signal attenuation due to environmental effects along the transmission path and the system itself [1, 13].

The external noise power included in our simulation, $S_{Noise}(t)$, which in HF band may arise from a combination of atmospheric, galactic and man-made sources [15], is determined based on the signal to

noise ratio (SNR). This noise is assumed as a stationary Gaussian white process with zero mean and adjustable noise power through SNR.

First-order backscattering of sea clutter is considered, that is the radar cross section of the sea surface (σ_C) due to simple backscattering by Bragg waves. These waves impose a Doppler shift f_B (or $\omega_B = 2\pi f_B$) given by

$$f_B = \pm\sqrt{\frac{g f_C}{\pi c}} = \pm 0.102\sqrt{f_c} \tag{5}$$

where f_c is in MHz and g is the acceleration due to gravity. $S_{Clutter}$ results then

$$S_{Clutter}(t) = A\,\sigma_C\,P_T\,G_R\,G_T\,u(t-\tau_R)\,m(t)\,e^{j\omega_C t \pm j\omega_B t} \tag{6}$$

similar to the target echo, but with the corresponding radar cross section and being emitted by the whole scanned area.

The searching area scanned by the transmitter is divided into dwell illumination regions (DIR), which in turn are divided into k resolution cells, shown schematically in [5]. The transmission-reception process is repeated N times per cell. The obtained Nk signals are arranged within a two-dimensional matrix *M*, in order to proceed with the digital signal processing.

The digital signal processing, which involves a set of techniques to remove clutter and noise, and to cope with attenuation, consists in the following steps:

1. Matched adaptive filtering, with a self-adjusting transfer function, which in our case is a conjugated time reversed version of the transmitted signal to maximize SNR.
2. A time-domain window function applied to each row in M to reduce edge effects which result in spectral leakage in the Fast Fourier Transform, FFT. The Kaiser window is used with β parameter equal to 31.
3. FFT applied to each row in *M* to obtain the total spectrum of the analyzed resolution cell and get the velocity information.
4. Filtering of the "artificial" clutter by subtracting a clutter map. This map results from the average spectrum of four consecutive DIR scans.
5. Target detection using a Cell Averaging Constant False Alarm Rate (CA-CFAR) in 2-D. The false alarm probability, P_{FA}, is the input parameter that can be modified in our simulation. This method permits an automatic determination of an adaptive threshold to finally detect, or not, a target.

Radar Output

After the whole process, the simulation tool output consists on a range-Doppler spectrum together with the target range and velocity values. This block yields the spectrum plots and list the target position and velocity.

SENSITIVITY ANALYSIS

Each module, or block, in the OTHR simulation tool has a set of variable parameters that can be evaluated through SA. Those related to clutter and noise simulation, their filtering processes, target radar cross section, and digital signal processing affect in particular the target detection ability. The ray tracing module, on the other hand, determines the target location, and/or the scanned cell position, in terms of geographic latitude and longitude. In order to determine the sensitivity of our simulation tool we analyze its detection ability for varying f_c and v, from a specific initial scenario described in Tables 1, 2 and 3.

Table 1 describes the transmitter, that is a sky-wave OTHR, and the transmitted signal characteristics. The OTHR, whose geographic position is shown in Figure 2, is located at Chubut

province's coast, Argentina. Tables 2 and 3 describe the environment and target specifications used in the initial scenario.

A DIR area enclosing the target is considered, with a minimum range of 1300 km and maximum of 1600 km. This area is divided into resolution cells along the range only, for a fixed azimuth direction containing the target. The range resolution, ΔR, is given by c/2B, which for B = 10 kHz, results 15 km. This implies 20 resolution cells along the range coverage.

The remaining specification needed to run the simulation are the following: m(t): binary phase shift keying (BPSK) with 13-bit Barker code, N = 270, PRF = 40 Hz, $P_{FA} = 10^{-8}$.

According to N and PRF values, the coherent processing interval (N/PRF) is 6.8 seconds, and the frequency resolution results 0.15 Hz [1].

A superheterodyne receiver is considered whose main functions are: baseband shift of the signal spectrum and SNR and SCR (Signal to Clutter Ratio) improvements.

Figure 2. OTHR geographic location in Argentina (green region), South America, together with the search area and DIR.

The values of SNR and SCR are defined by

$$\text{SNR [dB]} = (P_T + G_T + G_R - \text{Atte}_{\text{round trip}} + \sigma_T) - P_{\text{noise}} \quad (7)$$

$$\text{SCR[dB]} = (P_T + G_T + G_R - \text{Atte}_{\text{round trip}} + \sigma_T) - (P_T + G_T + G_R - \text{Atte}_{\text{round trip}} + \sigma_C) = \sigma_T - \sigma_C \quad (8)$$

In our initial scenario the receiver SNR and SCR have mean values of -94 dB and -34 dB, respectively, which are typical values for OTH skywave radars. Figure 3 shows the range-Doppler spectrum output of this scenario simulation at three different stages of the digital signal processing, where range is indicated in terms of the resolution cell number. The target is detected at the 7th cell, that is at a distance between 1390 km (1300 km + 6 × 15 km) and 1405 km (1300 km + 7 × 15 km), with a Doppler frequency equal to 0.15 Hz, which implies a target velocity of 13.5 km/h. In this particular case, in addition to the target detection, there are six additional unwanted detections.

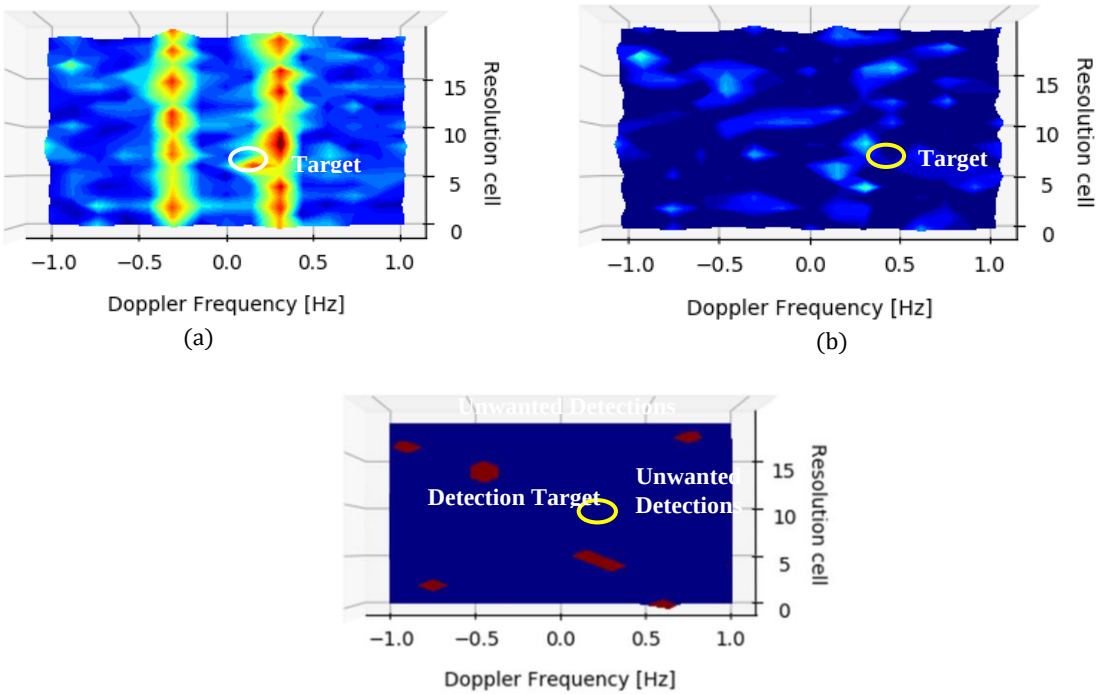

Figure 3. Range-Doppler display considering parameters given in Tables 1–3 at different stages of the digital signal processing: (a) after steps 1, 2 and 3 (matched adaptive filtering, reduction of edge effects, and FFT application) where blue indicates no power received, and red corresponds to maximum power; (b) after step 4 (filtering of the "artificial" clutter by subtracting a clutter map); and (c) after step 5 (Cell Averaging Constant False Alarm Rate (CA-CFAR) in 2-D) where the four red areas correspond to positive detections. Yellow line encircles the "real" target.

The errors in the target's range and velocity are acceptable for this type of radar, which is an early warning system and thus high precision is not required. To decrease the number of false detections, the process of searching should be repeated two or three times, and consider as a target detection the common red areas in all the repetitions. Detections which do not correspond to a "true" target will randomly change positions in the range-Doppler spectrum, and therefore are not expected to survive along repetitions.

SA of Radar Cross-sections to changes in f_c

Among the variables in our OTHR simulation tool that depend on f_c (σ_T, σ_c, SNR, SCR, f_B, and f_D), the sensitivity of three of them is analyzed: σ_T, SNR and SCR. Despite σ_c also varies with f_c, it is considered here as an independent modifiable parameter. The selection of f_c depends on the frequency channel that is free of other HF band users and the optimum values that maximize SNR, which in skywave OTHR would be around the maximum usable frequency.

Figure 4 shows SNR and SCR in terms of f_c, keeping constant all other parameters of the simulation. Along feasible f_c values (between ~3 and ~25 MHz), SNR and SCR vary both in a range of ~10 dB amplitude. A general improvement can be observed for increasing f_c, except between ~10 and ~15 MHz where SNR present a rather strong decrease. Below 3 MHz the DSP does not work adequately due to the improvement limitations of the receiver's SNR and SCR.

In the case of σ_T, polarization considerations should be also made. The transmitted signal has a polarization that is known when it leaves the transmitter, as indicated in Table 1; but, when this signal

propagates through the ionosphere its polarization becomes unknown due to the Earth's magnetic field effect on ionospheric refractive index. Even though it may be possible to estimate the polarization change along the ionospheric ray-path, we consider σ_T mean value between the horizontal and vertical polarization extreme cases. Another factor affecting σ_T is the azimuth between the transmitter-target direction and the target orientation (assuming the more general 90º case that is non-azimuth symmetry). As the target moves along its trajectory this azimuth angle will change. But, for our purposes an average response is enough. Figure 5 shows σ_T in terms of f_C, where all other parameters of the simulation are kept constant.

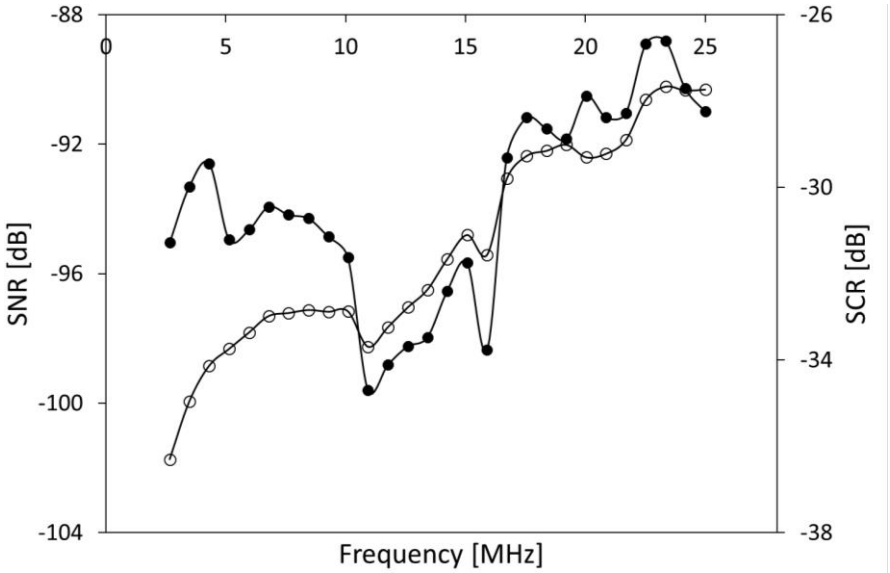

Figure 4. Signal to Noise Ratio, SNR [dB] (filled circle), and Signal to Clutter Ratio, SCR [dB] (empty circle), at the receiver in terms of the carrier frequency, f_c [MHz]. Note: circles indicate the f_c at which the simulation was run.

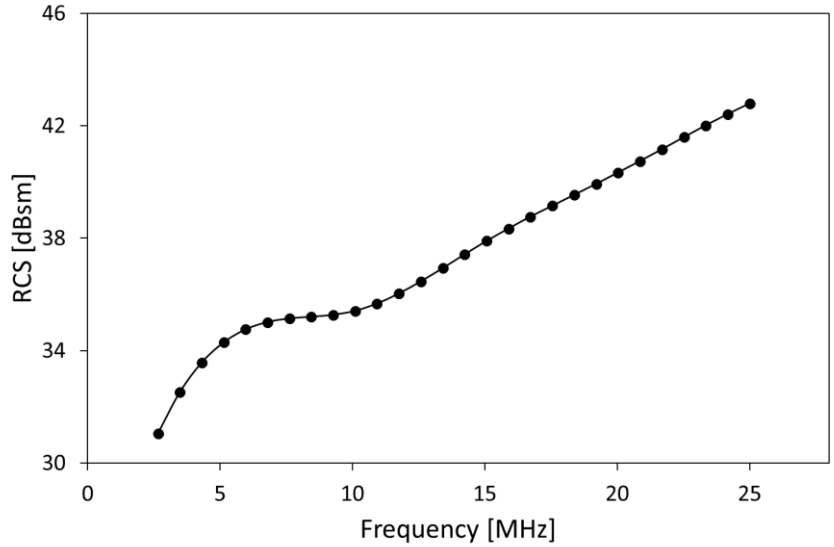

Figure 5. Target radar cross section, σ_T, or RCS, in terms of the carrier frequency, f_c [MHz].

As in SNR and SCR cases, σ_T increase for increasing f_c. It is worth noting that variations in σ_T affect SNR. Thus, there is a lowest σ_T value below which SNR would be below the DSP required threshold to adequately detect the target.

SA to Changes in v

The parameter that clearly depends on v is the target Doppler frequency f_D, which is a direct function of this variable. The purpose of a sensitivity analysis in this case is to determine thresholds to properly distinguish it from f_B. Figure 6 shows f_B and f_D in terms of fc considering three velocities. The difference between f_B and f_D, which is plot in Figure 7, depends on f_c. Depending on the target velocity, there is an f_c value which results in f_B and f_D being equal.

As an example, considering f_c = 6 MHz, the Doppler and Bragg frequencies are equal for a target velocity v = 42 km/h, as can be noticed in Figure 8. In this case the target should overcome step 4 of the DSP in all the repetitions in order to isolate its position in the range-Doppler spectrum.

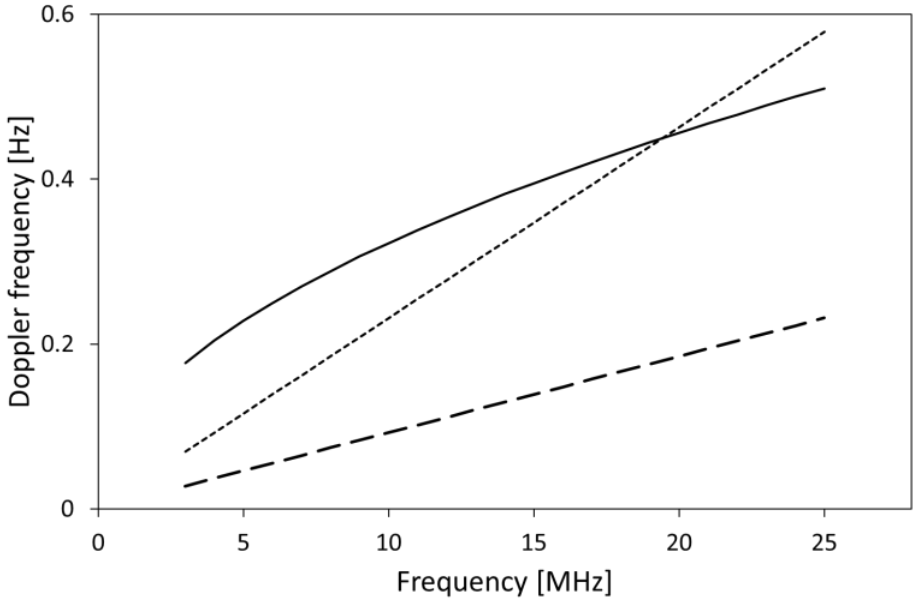

Figure 6. Doppler frequencies: f_B [Hz] (solid line) and f_D [Hz] for target velocities 10 km/h (dashed line) and 25 km/h (dotted line) in terms of carrier frequency, f_c [MHz].

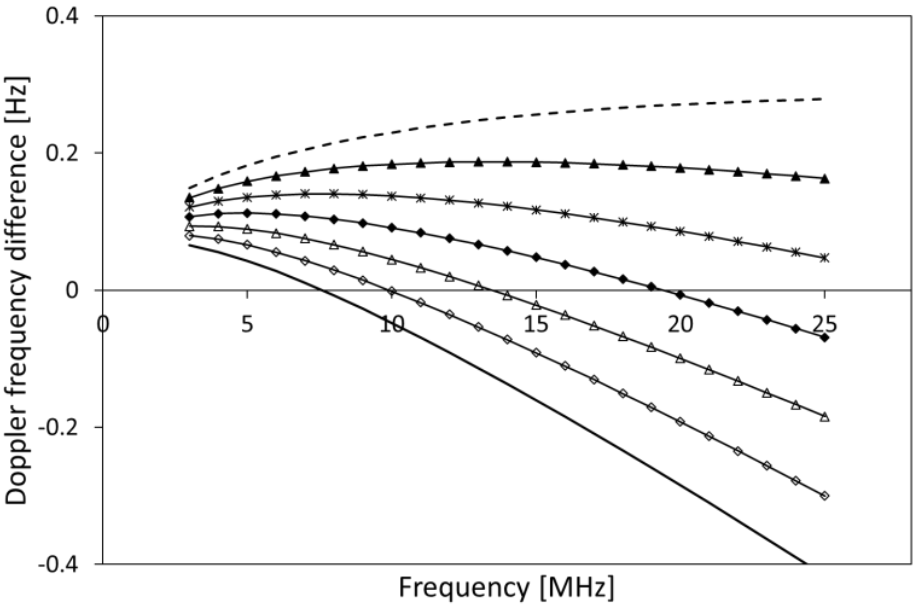

Figure 7. Doppler frequencies difference (f_B-f_D) [Hz] in terms of carrier frequency, f_c [MHz] for different target velocities, v: 10 km/h (dashed line), 15 km/h (filled triangle), 20 km/h (asterisk), 25 km/h (filled diamond), 30 km/h (empty triangle), 35 km/h (empty diamond), and 40 km/h (solid line).

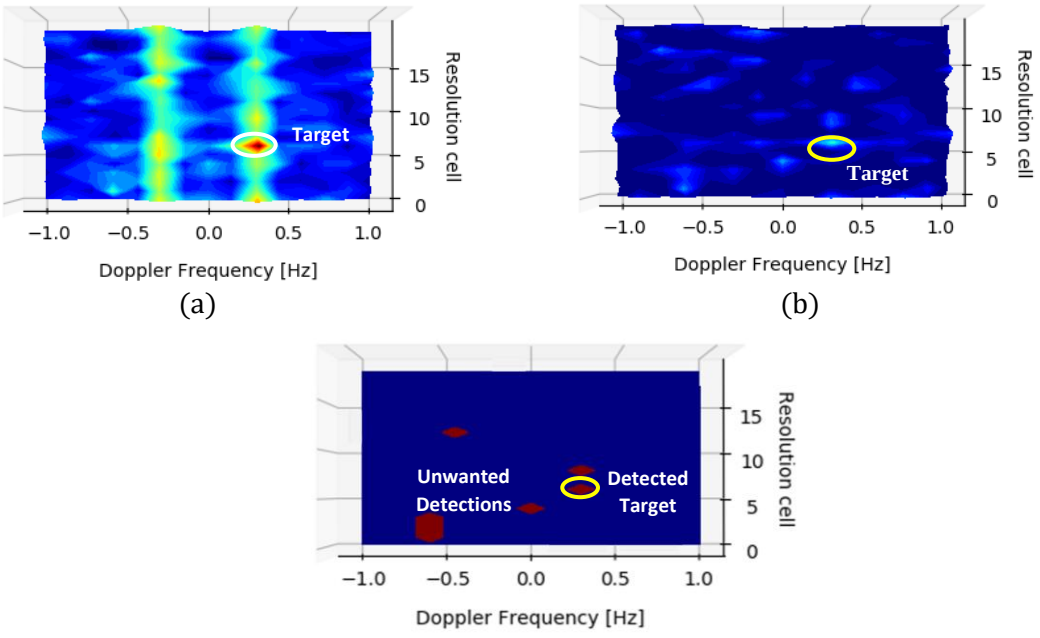

Figure 8. As in Figure 3 considering $f_B = f_D$.

DISCUSSION

The simulation of an OTHR operation has several parameters involved which affect the radar ability to detect accurately a real target. These parameters, in turn, are not fully independent. The OTHR simulation tool described in Saavedra et al. [4, 5] was used to evaluate the radar behavior and performance through a sensitivity analysis for varying f_c and v. f_c is a key parameter since, in addition to its effect on the ray path through the ionosphere, it determines σ_T, σ_c, SNR, SCR, f_B, and f_D, while v directly modifies f_D. However, in this last case, since the detection process depends on the ability to differentiate an echo from noise and clutter, even though v may affect only one radar parameter (f_D), it is the relation to other magnitudes which will result in a correct detection or not.

In the case of f_c, increasing values result in general SNR, SCR and σ_T improvements. Only in SNR case a worsening is noticed in the 10-15 MHz range, which is due to ray-path differences. Higher f_c implies longer paths to reach the target. If it is fixed at a certain position, a higher elevation angle would be needed since the height at which ionospheric reflection occurs will be higher (due to the ionosphere secant law). In the present case, where the elevation angle is fixed, the ray path reaches the Earth (where the target is assumed to be) in a farther position, in addition to the increase ray path due to the higher reflection height. Thus, the geometric attenuation L_g should increase while the target signal echo intensity should decrease. This also happens to the noise echo (its power decreases for longer ray-paths). In fact, the linear correlation coefficient between the ground range and the target and noise power is -0.91 and -0.84 respectively. However, the power ratio, that is SNR, increases and behaves like the ground range at large scales. Its correlation with the ground range is positive as expected, but low, being 0.34. The correlation of SNR with f_c increases to 0.63 which allow us to conclude that SNR is sensitive to f_c, even though not through a simple direct association. In the clutter case, its variation with f_c is more stable with a correlation coefficient of 0.93. So it is more sensitive to f_c than SNR, as can be also deduced from Figure 4. The radar cross section, σ_T, is also highly sensitive to f_c, with a correlation of 0.96 (see Figure 5).

With respect to the target velocity, its variation affects the f_D-f_B resolution. For a fastest target, its position in the range-Doppler spectrum will coincide with f_B for higher f_c values as can be noticed from Figures 6 and 7. However, this should not be a problem as long as the SCR is high enough so as

not to be discarded by the DSP process after step 4, where the clutter map is subtracted from the range-Doppler spectrum output of the simulation. Since σ_T also increases with f_c it should not be a problem. There is compromise then between f_D-f_B, which is highly sensitive to v, and the ability of σ_T to overcome the clutter map subtraction.

CONCLUSION

A problem to consider in future works is the sensitivity to ionospheric conditions, which are highly variable, especially with the occurrence of travelling ionospheric disturbances, TIDs, that induce apparent range and azimuth motions. Since they are not included in the ionosphere model, these variations appear as true variations in ground range and azimuth. Even though our study does not include this particular analysis, the present sensitivity analysis may serve to include them as part of detection errors. OTH systems depends critically on realistic ionospheric modeling along with accurate and fast ray tracing algorithms. Another problem to consider in future works is the availability of HF free channels which can significantly reduce the radar frequency options, and the target type since aircraft and ship detection, for example, have different optimal radar parameters each, including the operating frequency, emission bandwidth, PRF and coherent integration time.

Acknowledgements

This work was supported by PIDDEF 03-2020 (Programa de Investigación y Desarrollo para la Defensa) granted by Argentina Ministry of Defense (MINDEF).

REFERENCES

1. Fabrizio GA. High frequency over-the-horizon radar: fundamental principles, signal processing, and practical applications. New York, USA: McGraw-Hill; 2013.
2. Francis DV, Cervera MA, Frazer GJ. Performance Prediction for Design of a Network of Skywave Over-the-Horizon Radars. IEEE Aerospace and Electronic Systems Magazine 2017; 32: 18–28.
3. Thayaparan T, Marchioni J, Kelsall A, et al. Improved frequency monitoring system for sky-wave over-the-horizon radar in Canada. Geosci. Rem. Sens. Lett. IEEE 2019; 17: 606–609.
4. Saavedra Z, Argota JN, Cabrera MA, et al. A New Approach to OTH Main Parameters Determination. Radioengineering 2019; 28: 643–650.
5. Saavedra Z, Zimmerman D, Cabrera MA, et al. Sky-wave over-the-horizon radar simulation tool. IET Radar, Sonar & Navigation 2020; 14: 1773–1777.
6. Pianosi F, Beven K, Freer J, et al. Sensitivity analysis of environmental models: A systematic review with practical workflow. Environmental Modelling & Software 2016; 79: 214–232.
7. Razavi S, Jakeman A, Saltelli A, et al. The Future of Sensitivity Analysis: An essential discipline for systems modeling and policy support. Environmental Modelling & Software 2021; 137: 104954.
8. Headrick JM, Skolnik MI. Over-the-Horizon radar in the HF band. Proceedings of the IEEE 1974; 62: 664–673.
9. Jones RM, Stephenson JJ. A versatile three-dimensional ray tracing computer program for radio waves in the ionosphere. OT Report, 75–76. Department of Commerce, Office of Telecommunication. Washington (USA): U.S. Government Printing Office, 1975.
10. Bilitza D. IRI the International Standard for the Ionosphere. Adv. Radio Sci. 2018; 16: 1–11.
11. Thébault E, Finlay CC, Beggan C, et al. International Geomagnetic Reference Field: the 12th generation. Earth, Planets and Space 2015; 67: 79.
12. Zolesi B, Cander LR. Ionospheric Prediction and Forecasting. Berlin, Germany:Springer, Berlin; 2014.
13. ITU. Method for the Prediction of the Performance of HF Circuits ITU-R P.533-13. Geneva, Switzerland: International Telecommunication Union (ITU); 2015.
14. Billingsley JB. Low-Angle Radar Land Clutter. Measurements and Empirical Models. New York, USA: William Andrew Publishing; 2002.
15. ITU. Recommendation ITU-R P.372-15, Radio noise, P Series, Radiowave propagation. Geneva, Switzerland: International Telecommunication Union (ITU); 2021.

